Advanced Journal of Chemistry, Section A, 2024, 7(2), 146-162

Advanced Journal of Chemistry, Section A

journal homepage: www.ajchem-a.com

Original Research Article

Molecular Modeling Insights into Bioactivities of Head-to-Tail Cyclic Peptides: Potential Sedoheptulose-7-Phosphate Isomerase Inhibitors

Abel Kolawole Oyebamiji[1]*, Sunday A. Akintelu[2], Banjo Semire[3], Adesoji Alani Olanrewaju[1], Emmanuel T. Akintayo[4], Cecillia O. Akintayo[5], Habibat Omolara Adubiaro[5], Oluwakemi Ebenezer[6], Jonathan O. Babalola[1]

[1] *Department of Chemistry and Industrial Chemistry, Bowen University, Iwo, Osun State, Nigeria*
[2] *School of Chemistry and Chemical Engineering, Beijing Institute of Technology, Beijing, China*
[3] *Department of Pure and Applied Chemistry, Ladoke Akintola University of Technology, Ogbomoso, Oyo State, Nigeria*
[4] *Department of Chemistry, Ekiti State University, Ado-Ekiti, Nigeria*
[5] *Department of Chemistry, Federal University, Oye-Ekiti, Nigeria*
[6] *Department of Physics, University of Alberta, Edmonton, Canada*

ARTICLEINFO

Article history

Submitted: 28 September 2023
Revised: 30 October 2023
Accepted: 26 November 2023
Available online: 27 November 2023

Manuscript ID: AJCA-2309-1426
Checked for Plagiarism: **Yes**
Language editor:
Dr. Fatimah Ramezani
Editor who approved publication:
Dr. Mehmet Ozgur Seydibeyoglu

DOI: 10.48309/ajca.2024.418437.1426

KEYWORDS

Peptides
Bioactive
Inhibitors
Modeling
Bacteria

ABSTRACT

The biological activity and properties of fourteen cyclic peptides were investigated using *in silico* approach. The predicted features for the studied compounds using 6-31G* via Spartan 14 software were lipophilicity, the highest occupied molecular orbital energy, the lowest occupied molecular orbital energy, HOMO/LUMO energy gap, dipole moment, molecular weight, and polar surface area. The descriptors obtained perfectly described the activities of the studied ligands. Likewise, the studied ligands were docked against sedoheptulose-7-phosphate isomerase [PDB id: 2x3y] and it was observed that all the ligands examined in this work have higher binding affinity than the ceftazidime (referenced drug) except compound **9** and **12**. The predicted compounds proved to have higher binding affinities than the referenced compound and these were further confirmed using molecular dynamic simulation as well as pharmacokinetics studies.

GRAPHICALABSTRACT

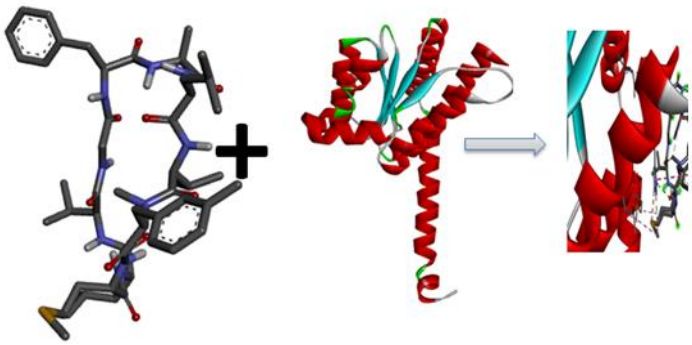

* Corresponding author: Oyebamiji, Abel Kolawole
✉ E-mail: abeloyebamiji@gmail.com
© 2024 by SPC (Sami Publishing Company)

Introduction

Burkholderia pseudomallei is the Gram-negative bacterium that cause infection termed "Melioidosis" [1, 2]. It widely dominates soil as well as water surface and could easily be found in Asia and Australia continents [3]. It is a gram-negative organism which has been declared to be a major cause of death in Thailand as well as other neighboring countries in Asia and Australia continents [4]. In several developing countries, *B. pseudomallei* have been observed to be resistant to some drugs (penicillin and gentamicin) which were considered as a usual way of treating bacterial [5]. The length and diameter of *B. pseudomallei* were reported to be between 2 µm and 5 µm as well as 0.4 µm and 0.8 µm, respectively [6]. *B. pseudomallei* uses flagella for self-momentum and it has the ability to grow in locations containing betaine as well as arginine [7]. Therefore, series of enzymes in *B. pseudomallei* has being the target for drug design analysis. The role played by Sedoheptulose -7-phosphate in *B. pseudomallei* has been considered as crucial and researchers has used it as the target in developing *B. pseudomallei* inhibitors [8]. It was reported in several articles to be transitional agent in pentose phosphate pathway [9,10]. According to Taylor *et al.* (2008), transketolase was reported to formulate Sedoheptulose -7-phosphate which was further used by transaldolase [11]. Furthermore, this enzyme helps in catalyzing D-sedoheptulose-7-phosphate in order to produce D-glycero-D-manno-heptose 7-phosphate. Gram-negative bacteria use D-sedoheptulose-7-phosphate isomerase to produce ADP-L-glycero-β-D-manno-heptose [12]. Moreover, drug-like compound like Ceftazidime has been engaged to hinder the activity of sedoheptulose-7-phosphate isomerase so as to destroy the role of *B. pseudomallei* among human and animals [13], yet lasting solution is still required to combat this menace amidst the living being.

Head-to-tail cyclic peptides are combinations of peptides in cyclic format. The formation of peptides requires joining the head and the tail of peptide to amide bond [14]. According to many researchers, it was observed that naturally occurring peptides played serious therapeutic roles in combating several diseases and this kind of biomolecules has become a major tool to many researchers in developing drug-like molecule [14-16]. As reported by Román-Hurtado *et al.*, cyclic peptides possess high binding affinity, specificity, and selectivity as well as low toxicity [17]. Therefore, this work is aimed at identifying the amino acid residues involved in the interaction between the studied peptides and sedoheptulose-7-phosphate isomerase [PDB id: 2x3y] [18] as well as observing the roles of the descriptors obtained from the optimized studied cyclic peptide.

Methodology

Ligand Optimization and Preparation

Two dimensional structures of the studied head-to-tail cyclic peptides which were obtained from the research carried out by Li *et al.* (2022) [19] were carefully drawn using Chemdraw ultra 12.0 version and were converted to 3-dimensional design via Spartan'14 [20, 24]. The sketched structures were displayed in ball and spoke model which were minimized before subjected to optimization. The optimization calculation was achieved using density functional theory, B3LYP, 6-31G* as basis set and the calculation was performed in vacuum. According to Jacquemin *et al.* (2008), the correctness of density functional theory (DFT) calculations has been linked to the chosen functional and basis sets [25] and the chosen functional (B3LYP) and 6-31G* (basis set) have been ascertained to be adequate for calculating the excitation properties of drug-like compounds. Thus, the addition of other diffuse functions in basis sets has insignificant effects on the electron density [26-

28]. It was observed that the calculation started from current geometry and the total charge and unpaired electrons were set to neutral and zero (0), respectively before final submission for optimization.

The IUPAC name of the peptides under investigation presented in Table 1.

Table 1. IUPAC name and Investigated head-to-tail cyclic peptides

IUPAC name	2-Dimensional Structure	3-Dimensional Structure
(3*S*,6*S*,9*S*,12*S*)-12-benzyl-3-isobutyl-9-(3-methylbenzyl)-6-(2-(methylthio)ethyl)-1,4,7,10,13-pentaazacyclopentadecane-2,5,8,11,14-pentaone (**1**)	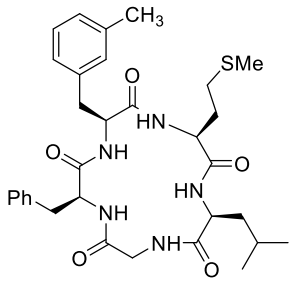	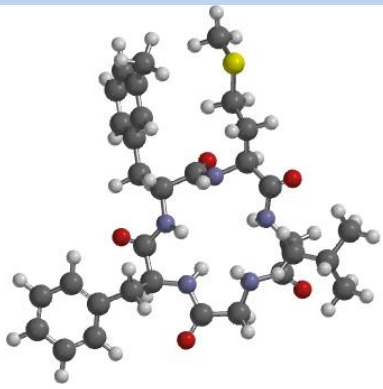
(6*S*,9*S*,12*S*,15*S*,20a*R*)-6-benzyl-15-isobutyl-9-(3-methylbenzyl)-12-(2-(methylthio)ethyl)tetradecahydropyrrolo[1,2-a][1,4,7,10,13,16]hexaazacyclooctadecine-1,4,7,10,13,16-hexaone (**2**)	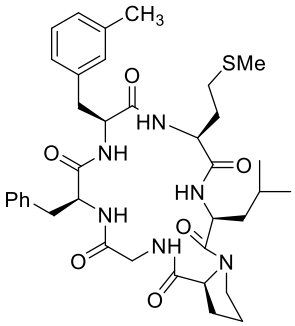	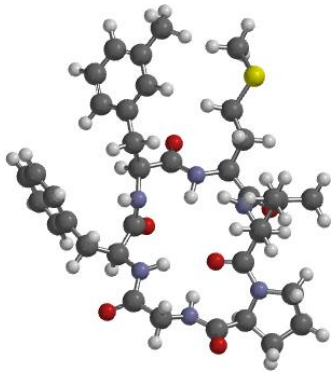
N-(4-((6*S*,9S,12*S*,15*S*,20a*R*)-6-benzyl-15-isobutyl-12-(3-methylbenzyl)-1,4,7,10,13,16-hexaoxoicosahydropyrrolo[1,2-a][1,4,7,10,13,16]hexaazacyclooctadecin-9-yl)butyl)-4-methylbenzenesulfonamide (**3**)	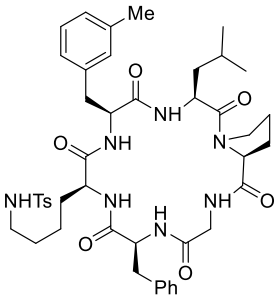	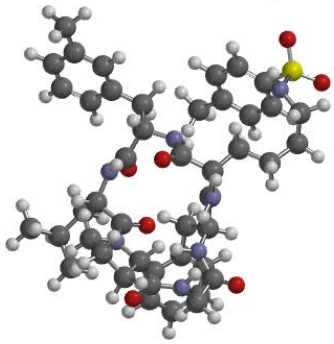
(3*S*,6*S*,9*S*,12*S*,15*S*)-15-benzyl-3-isobutyl-6-isopropyl-12-(3-methylbenzyl)-9-(2-(methylthio)ethyl)-1,4,7,10,13,16-hexaazacyclooctadecane-2,5,8,11,14,17-hexaone (**4**)	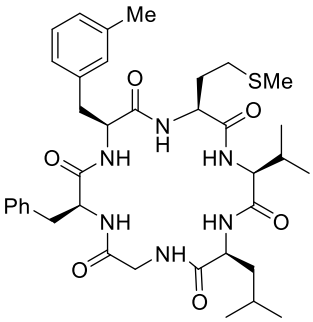	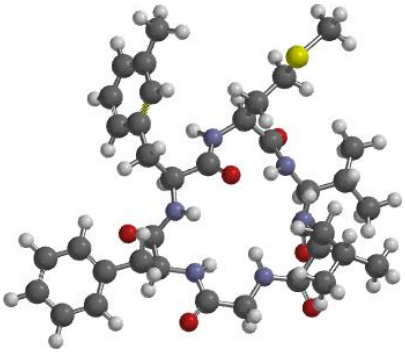

IUPAC name	2-Dimensional Structure	3-Dimensional Structure
methyl 4-(((2*S*,5*S*,8*S*,11*S*,17*S*)-17-benzyl-11-isobutyl-8-isopropyl-5-(2-(methylthio)ethyl)-3,6,9,12,15,18-hexaoxo-1,4,7,10,13,16-hexaazacyclooctadecan-2-yl)methyl)benzoate (**5**)	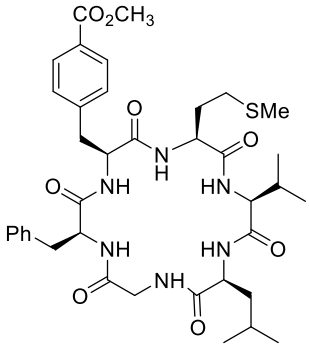	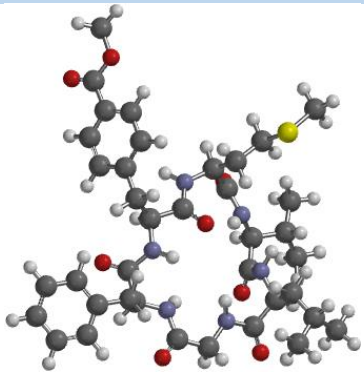
(3S,6S,9S,12S,15S)-15-benzyl-12-(4-bromobenzyl)-3-isobutyl-6-isopropyl-9-(2-(methylthio)ethyl)-1,4,7,10,13,16-hexaazacyclooctadecane-2,5,8,11,14,17-hexaone (**6**)	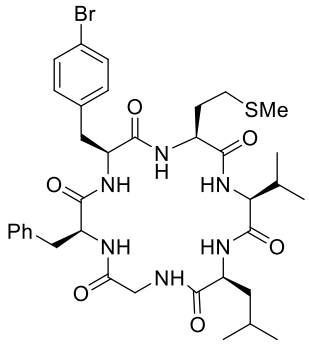	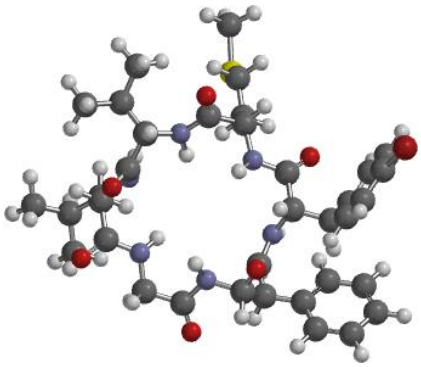
N-(4-(((2S,5S,8S,11S,17S)-17-benzyl-11-isobutyl-8-isopropyl-5-(2-(methylthio)ethyl)-3,6,9,12,15,18-hexaoxo-1,4,7,10,13,16-hexaazacyclooctadecan-2-yl)methyl)phenyl)acetamide **(7)**	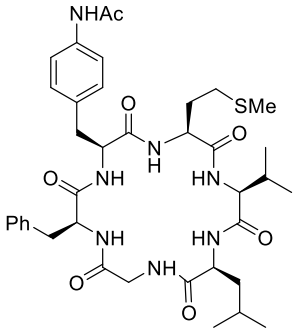	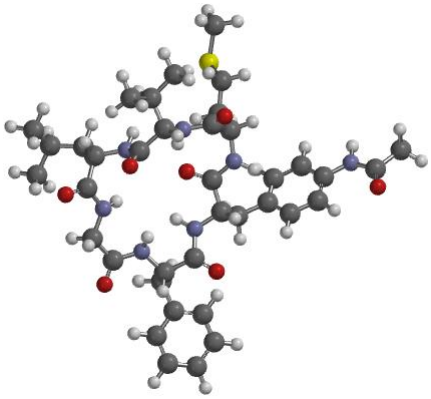
(3*S*,9*S*,12*S*,15*S*,18*S*)-3-benzyl-9-isobutyl-12-isopropyl-1-methyl-18-(3-methylbenzyl)-15-(2-(methylthio)ethyl)-1,4,7,10,13,16-hexaazacyclooctadecane-2,5,8,11,14,17-hexaone (**8**)	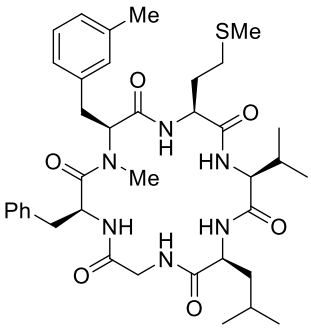	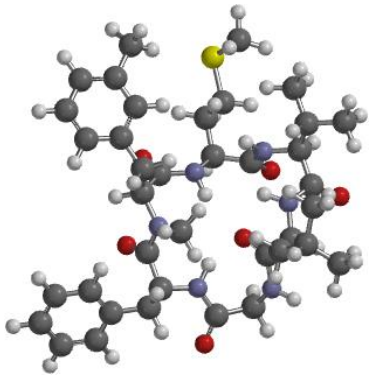

IUPAC name	2-Dimensional Structure	3-Dimensional Structure
(3*S*,6S,9*S*,12R,15*S*,18*S*,21*S*)-3,12-dibenzyl-9,15-diisobutyl-21-(4-methoxybenzyl)-6-methyl-18-(2-(methylthio)ethyl)-1,4,7,10,13,16,19-heptaazacyclohenicosane-2,5,8,11,14,17,20-heptaone (**9**)	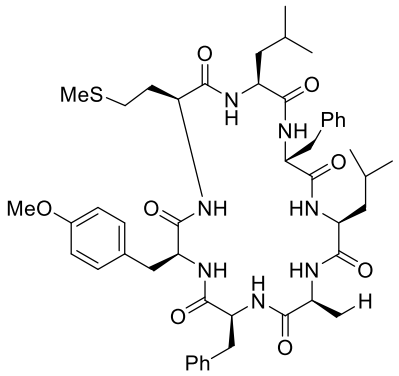	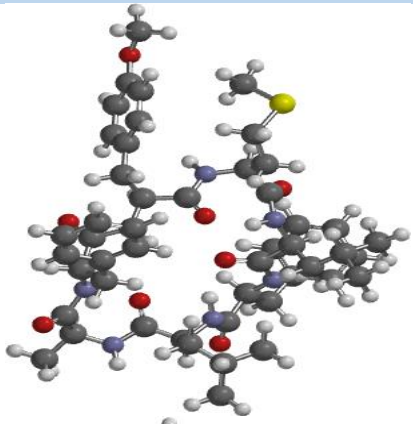
(3S,6R,9S,12S,15S,18S)-6,18-dibenzyl-3-isobutyl-9-isopropyl-15-(4-methoxybenzyl)-12-(2-(methylthio)ethyl)-1,4,7,10,13,16,19-heptaazacyclohenicosane-2,5,8,11,14,17,20-heptaone (**10**)	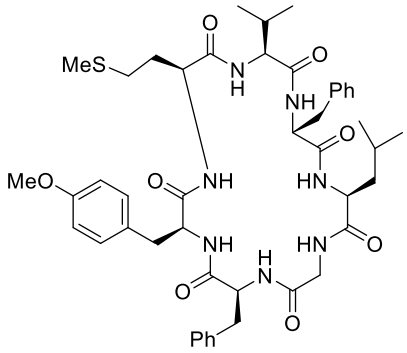	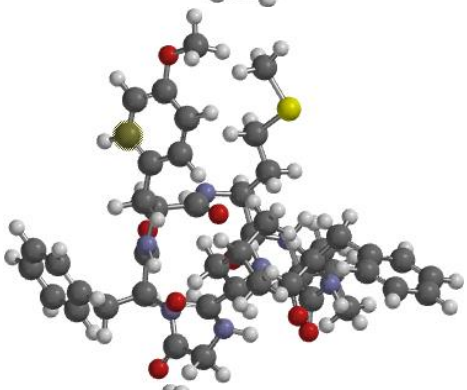
N-(4-((2S,8S,11S,14S,17S,20R)-8,20-dibenzyl-17-isobutyl-11-(4-methoxybenzyl)-14-(2-(methylthio)ethyl)-3,6,9,12,15,18,21-heptaoxo-1,4,7,10,13,16,19-heptaazacyclohenicosan-2-yl)butyl)-4-methylbenzenesulfonamide (**11**)	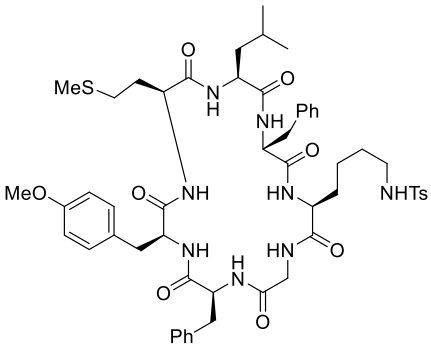	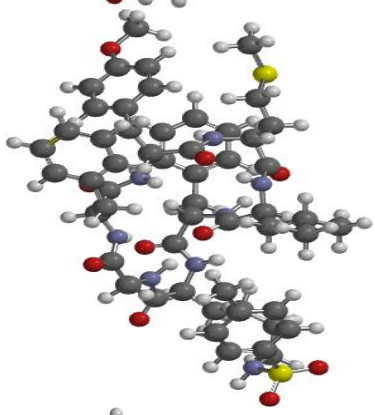
(3S,6R,9S,12S,15S,18S)-18-benzyl-6-((benzyloxy)methyl)-3-isobutyl-9-isopropyl-15-(4-methoxybenzyl)-12-(2-(methylthio)ethyl)-1,4,7,10,13,16,19-heptaazacyclohenicosane-2,5,8,11,14,17,20-heptaone (**12**)	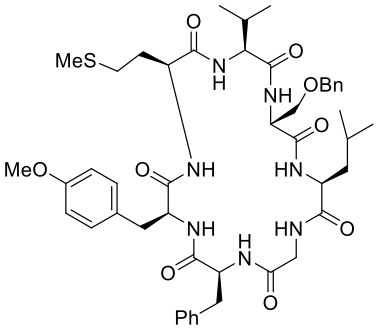	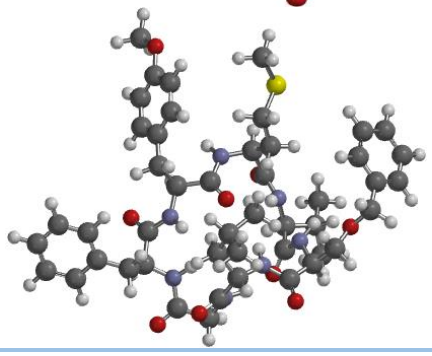

IUPAC name	2-Dimensional Structure	3-Dimensional Structure
(3S,6S,9S,12S,15S,18S,21R)-3,18-dibenzyl-15,21-diisobutyl-6-isopropyl-12-(4-methoxybenzyl)-9-(2-(methylthio)ethyl)-1,4,7,10,13,16,19,22-octaazacyclotetracosan-2,5,8,11,14,17,20,23-octaone (**13**)	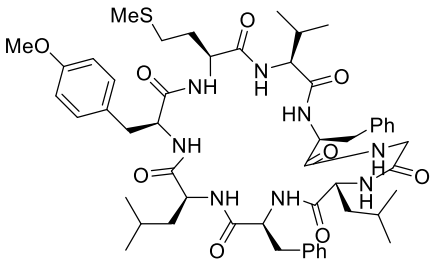	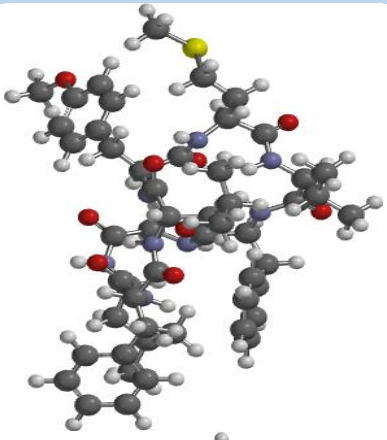
(3S,6S,9S,12S,18S,21S,24S,27S)-12-benzyl-6,21-diisobutyl-3,18-diisopropyl-1,9-dimethyl27-(3-methylbenzyl)-24-(2-(methylthio)ethyl)-1,4,7,10,13,16,19,22,25-nonaazacyclohep-tacosane-2,5,8,11,14,17,20,23,26-nonaone (**14**)	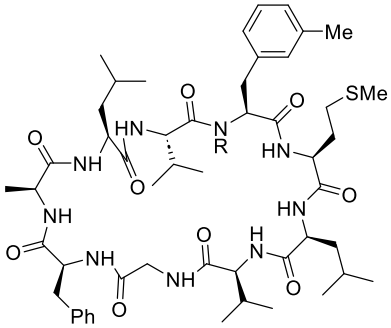	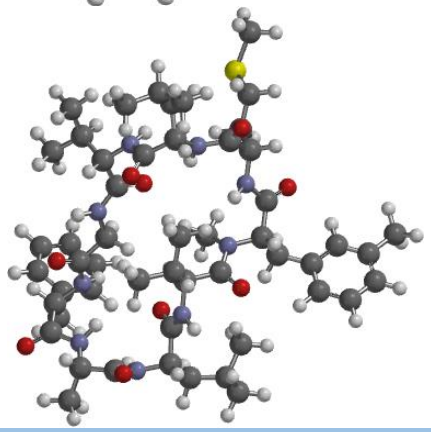

Molecular Docking Exploration

The investigation on understanding the role of each atom in the studied compounds linked to the amino acid residues in the studied protein (sedoheptulose-7-phosphate isomerase [PDB id: 2x3y]) [18] were executed using docking methods. The software used was pymol 1.7.4.4, Autodock tool 1.5.6, Discovery studio visualizer and Autodock vina [29-33]. Sedoheptulose-7-phosphate isomerase was downloaded from protein data bank and the sequence length of the downloaded protein was observed to be 219. The downloaded protein was screened and every other entity (Zn^{2+}) downloaded with the studied protein was removed using discovery studio software.

The process of locating the active site of the studied receptor involved the addition of appropriate hydrogen and kollman charges to the screened receptor before saving it in .pdbqt format using AutoDock Tool software. The Grid dimension of 30, 30, and 30 (X, Y, and Z dimension) as size and the obtained values for the center in X = -30.454000, Y = 69.580000 and Z = -7.376000 dimension were used for identifying the active site in the studied receptor (Figure 1). Furthermore, nine configurations were observed for each of the docked complex and the best scoring position of individual complex according to the calculated scoring was selected and subjected to visualization using discovery studio visualizer.

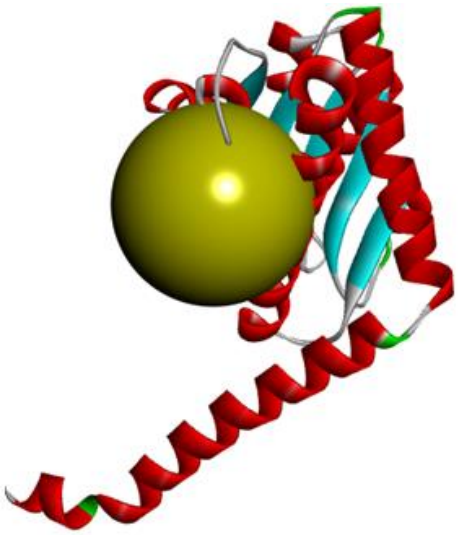

Figure 1. Screened Sedoheptulose-7-phosphate isomerase with active site identified.

Molecular Dynamic Simulation (MDS) Study

In this work, the compound ((3S,6S,9S,12S,18S,21S,24S,27S)-12-benzyl-6,21-diisobutyl-3,18-diisopropyl-1,9-dimethyl27-(3-methylbenzyl)-24-(2-(methylthio)ethyl)-1,4,7,10,13,16,19,22,25-nonaazacyclohep- -tacosane-2,5,8,11,14,17,20,23,26-nonaone (**14**)) with the highest binding affinity was subjected to molecular dynamic simulation study with Charmm36m as force field embedded in Gromacs software [34]. The stability of the studied compound was achieved during 100ns simulation time and the studied complexes systems were established with the help of TIP3P water molecule in an orthorhombic box of 10 Å on all sides.

Moreover, appropriate numbers of Sodium and Chloride ions were introduced to the simulating system so as to equipoise the charged system [35]. Both NVT and NPT ensemble were engaged during the simulation with the use of 100 nanoseconds with a 300 K and 1 bar in the studied system, respectively. Likewise, the use of CPPTRAJ module helped in analyzing molecular dynamics trajectories [36].

ADMET Analysis

The studied compound **14** **(**((3S,6S,9S,12S,18S,21S,24S,27S)-12-benzyl-6,21-diisobutyl-3,18-diisopropyl-1,9-dimethyl27-(3-methylbenzyl)-24-(2-(methylthio)ethyl)-1,4,7,10,13,16,19,22,25-nonaazacyclohep- -tacosane-2,5,8,11,14,17,20,23,26-nonaone) with highest binding affinity and the referenced compound (ceftazidime) were subjected to ADMET investigation which was executed using online software (ADMETlab software) [37]. The features of the selected compounds were obtained and reported.

Results and Discussion

Calculated Ligand Electronic Properties

The features of each optimized pharmacophore play vital role in chemical reactivity of such compound [38]. The role of highest occupied molecular orbital energy as well as the lowest unoccupied molecular orbital energy in chemical reactivity of any compounds requires a greater attention. The compound with utmost highest occupied molecular orbital energy value as well as lowest HOMO/LUMO energy gap value easily reacts with other compounds [39] and this shows it potential high level of reactivity. Thus,

(3S,6S,9S,12S,15S,18S,21R)-3,18-dibenzyl-15,21-diisobutyl-6-isopropyl-12-(4-methoxybenzyl)-9-(2-(methylthio)ethyl)-1,4,7,10,13,16,19,22-octaazacyclotetracosan-2,5,8,11,14,17,20,23-octaone (**13**) with -5.53eV (for highest occupied molecular orbital energy) and -4.60eV (for HOMO/LUMO energy gap) is expected to display high level of reactivity with other reacting molecules (Supp figure 1-14 and Supp Table 1).

Moreover, the reactivity of the studied compounds was determined via its ability to be a receiver of electron from other reacting molecules. Therefore, compound **5** with -1.66eV showed to be a potential compound to have the highest level of reactivity. Other features obtained from the optimized compounds are presented in Table 2.

Table 2. Calculated features of the studied compounds with 6-31G*

	E_H	E_L	EGap	DM	Mol Wei	Polar Sur. Area	Ovality	LOG P
1	-5.94	-0.55	5.39	3.60	609.792	116.603	1.87	-0.11
2	-5.73	-0.62	5.11	4.27	706.909	119.453	1.92	-0.55
3	-6.22	-0.67	5.55	9.85	858.074	158.695	2.02	-0.89
4	-6.28	-0.71	5.57	9.31	708.925	131.742	1.95	0.12
5	-6.31	-1.66	4.65	9.54	752.934	152.315	1.98	-0.54
6	-6.26	-0.67	5.59	6.81	773.794	140.463	1.96	0.08
7	-6.30	-0.85	5.45	11.73	751.950	155.487	1.98	-1.84
8	-5.90	-0.76	5.14	9.81	722.952	118.487	1.94	0.36
9	-6.02	-0.49	5.53	4.96	900.155	152.868	2.10	0.03
10	-6.06	-0.44	5.62	8.78	872.101	143.648	2.02	-0.81
11	-6.14	-1.00	5.14	14.11	1055.332	191.427	2.17	-1.53
12	-6.12	-0.70	5.42	13.11	902.127	158.861	2.10	-1.25
13	-5.53	-0.93	4.60	8.22	985.261	165.627	2.12	-0.23
14	-5.94	-0.70	5.24	6.42	1006.324	198.910	2.21	0.51

Note: E_H: The highest occupied molecular orbital energy; E_L: The lowest occupied molecular orbital energy; EGap: HOMO/LUMO energy gap; DM: Dipole moment; Mol Wei: Molecular weight; Polar Sur. Area: Polar surface area; LOG P: Lipophilicity

Molecular Docking Analysis

The investigated docking analysis exposed the potential inhibiting capacity of the studied functionalized peptides against sedoheptulose-7-phosphate isomerase [PDB id: 2x3y]. This method was engaged so as to recognize the energetic position of sedoheptulose-7-phosphate isomerase and get the topmost configuration of the peptide-sedoheptulose-7-phosphate isomerase complex. Table 3 lists the calculated binding affinity, amino acid residue as well as type of interaction which occur between the studied complexes.

The calculated binding affinity were -6.4 kcal/mol, -6.3 kcal/mol, -5.7 kcal/mol, -6.6 kcal/mol, -6.3 kcal/mol, -6.5 kcal/mol, -6.8 kcal/mol, -6.3 kcal/mol, -5.5 kcal/mol, -6.1 kcal/mol, -5.7 kcal/mol, -5.0 kcal/mol, -6.0 kcal/mol, and -7.1 kcal/mol for compound **1** to **14**. As provided in Table 3, it was detected that the reference compound proved to be active than compound **9** and **12** but other studied peptides (**1-8**, **10**, **11**, **13,** and **14**) proved to be more potent as potential sedoheptulose-7-phosphate isomerase inhibitors. According to Erazua *et al.*

(2021) [40], the lowest binding affinity signifies greatest tendency to inhibit receptor. Therefore (3S,6S,9S,12S,18S,21S,24S,27S)-12-benzyl-6,21-diisobutyl-3,18-diisopropyl-1,9-dimethyl27-(3-methylbenzyl)-24-(2-(methylthio)ethyl)-1,4,7,10,13,16,19,22,25-nonaazacyclohep-tacosane-2,5,8,11,14,17,20,23,26-nonaone (**14**) proved to have greatest potential strength to inhibit the target (Figure 2).

The exceptional activity of compound **14** in the active site of receptor to inhibit the studied target was observed to be due to the configuration of compound 14. As summarized in Table 2, the calculated molecular weight (1006.324 amu), polar surface area (198.910), ovality (2.21), and log P (0.51) was observed to enhance the inhibiting capacity of compound **14** than other studied compounds and the referenced drug. In this work, highest value of calculated molecular weight, polar surface area, ovality, and log P proved to aid the cytotoxicity of (3S,6S,9S,12S,18S,21S,24S,27S)-12-benzyl-6,21-diisobutyl-3,18-diisopropyl-1,9-dimethyl27-(3-methylbenzyl)-24-(2-(methylthio)ethyl)-1,4,7,10,13,16,19,22,25-nonaazacyclohep- -tacosane-2,5,8,11,14,17,20,23,26-nonaone (**14**).

The amino acid residue as well as the type of interaction observed between the studied complexes were Ala60; Met20; Leu179; Val180; Ala16; Ile13; and Glu176 (Conventional Hydrogen Bond, Pi-Sigma, Alkyl, and Pi-Alkyl) for compound **1**; His191; Phe 75; Ala74; Phe73; Gly 187; Ile184; and Leu 188 (Carbon hydrogen Bond, Pi-Sigma, Pi-Pi T-shaped, Alkyl, and Pi-Alkyl) for compound **2**; Arg72; Gly67; Ala66; and Ala84 (Carbon Hydrogen Bond, Pi-Sigma, Alkyl, and Pi-Alkyl) for compound **3**; Leu24; Met23; Leu188; Ala74; Phe73; and His183 (Pi-Sigma, Pi-Pi T-shaped, Alkyl, and Pi-Alkyl) for compound **4**; Leu30; Val33; Leu188; Phe73; Ala74; and Val180 (Pi-sigma, Pi-Sulfur, Alkyl, and Pi-Alkyl) for compound **5**; Glu68; Phe73; Ala74; Phe75; His191; and Glu68 (Pi-Anion, Pi-Pi Stacked, and Alkyl) for compound **6**; Met20; Met23; Val180; Leu179; His183; Phe73; Gly187; and Leu188 (Pi-Pi T-shaped, Amide-Pi Stacked, Alkyl, and Pi-Alkyl) for compound **7**; Ala 74; His191; Ile184; Val180; His183; and Leu188 (Pi-Pi T-shaped, Pi-Alkyl, and Alkyl) for compound **8**; Ala74; Met23; and Leu24 (Pi-Sulfur, Pi-Alkyl) for compound **9**; Ile-184; His 191; His183; Ala74; Phe73 (Pi-Sigma; Pi-Pi T-shaped, and Pi-Alkyl) for compound **10**; Ile184; Ala74; His183; Val180; and Leu179 (Conventional Hydrogen bond, Pi-Sigma; Alkyl; and Pi-Alkyl) for compound **11**; Ile184; Ala74; Phe75; His191 (Pi-Sigma, Pi-Sulfur, and Pi-Alkyl) for compound **12**; Ala84; Gly67; Ala60; Arg72; Glu68; Ser71; and Ala66 (Conventional Hydrogen bond, Carbon Hydrogen bond, Pi-Anion, Pi-Sigma, Alkyl, and Pi-Alkyl) for compound **13** and Ala74; Phe73; His 183; Leu179; Met20; Leu30; Val33; and Ile184 (Conventional Hydrogen bond; Pi-Sigma; Pi-Sulfur; Pi-Pi T-shaped, Alkyl, and Pi-Alkyl) for compound **14**.

As shown in Table 4, five (5) peptides were predicted which were derivatives of the parent compound used in the work. As depicted in Figure 2, five derivatives were attached to the parent compound before optimization using density functional theory. The predicted compounds were docked against sedoheptulose-7-phosphate isomerase (pdb id: 2x3y) and the obtained result were presented in Table 3. The calculated binding affinity for compound A to E were -6.5 kcal/mol, -6.3 kcal/mol, -6.6 kcal/mol, -6.4 kcal/mol, and -6.7 kcal/mol. Thus, all the predicted compounds were potent against the target and all the predicted compounds were effective potential anti- sedoheptulose-7-phosphate isomerase than the referenced drug (Figure 3). Also, compound **E** (-6.7 kcal/mol) with the highest binding affinity were subjected to further study.

Table 3. Calculated Scoring in kcal/mol

	Binding Affinity (kcal/mol)	Amino Acid Residues	Type of Non-bonding interaction
1	-6.4	Ala60; Met20; Leu179; Val180; Ala16; Ile13; and Glu176	Conventional Hydrogen Bond, Pi-Sigma, Alkyl, and Pi-Alkyl
2	-6.3	His191; Phe 75; Ala74; Phe73; Gly 187; Ile184; and Leu 188	Carbon hydrogen Bond, Pi-Sigma, Pi-Pi T-shaped, Alkyl, and Pi-Alkyl
3	-5.7	Arg72; Gly67; Ala66; and Ala84	Carbon Hydrogen Bond, Pi-Sigma, Alkyl, and Pi-Alkyl
4	-6.6	Leu24; Met23; Leu188; Ala74; Phe73; and His183	Pi-Sigma, Pi-Pi T-shaped, Alkyl, and Pi-Alkyl
5	-6.3	Leu30; Val33; Leu188; Phe73; Ala74; and Val180	Pi-sigma, Pi-Sulfur, Alkyl, and Pi-Alkyl
6	-6.5	Glu68; Phe73; Ala74; Phe75; His191; and Glu68	Pi-Anion, Pi-Pi Stacked, and Alkyl
7	-6.8	Met20; Met23; Val180; Leu179; His183; Phe73; Gly187; and Leu188	Pi-Pi T-shaped, Amide-Pi Stacked, Alkyl, and Pi-Alky
8	-6.3	Ala 74; His191; Ile184; Val180; His183; and Leu188	Pi-Pi T-shaped, Pi-Alkyl, and Alkyl
9	-5.5	Ala74; Met23; and Leu24	Pi-Sulfur, and Pi-Alkyl
10	-6.1	Ile-184; His 191; His183; Ala74; and Phe73	Pi-Sigma; Pi-Pi T-shaped, and Pi-Alkyl
11	-5.7	Ile184; Ala74; His183; Val180; and Leu179	Conventional Hydrogen bond, Pi-Sigma; Alkyl; and Pi-Alkyl
12	-5.0	Ile184; Ala74; Phe75; and His191	Pi-Sigma, Pi-Sulfur, and Pi-Alkyl
13	-6.0	Ala84; Gly67; Ala60; Arg72; Glu68; Ser71; and Ala66	Conventional Hydrogen bond, Carbon Hydrogen bond, Pi-Anion, Pi-Sigma, Alkyl, and Pi-Alkyl
14	-7.1	Ala74; Phe73; His 183; Leu179; Met20; Leu30; Val33; and Ile184	Conventional Hydrogen bond; Pi-Sigma; Pi-Sulfur; Pi-Pi T-shaped, Alkyl, and Pi-Alkyl
ref	-5.6	-	-

Ref: ceftazidime.

Table 4. Calculated Scoring in kcal/mol for predicted compounds

	Binding Affinity (kcal/mol)
A	-6.5
B	-6.3
C	-6.6
D	-6.4
E	-6.7

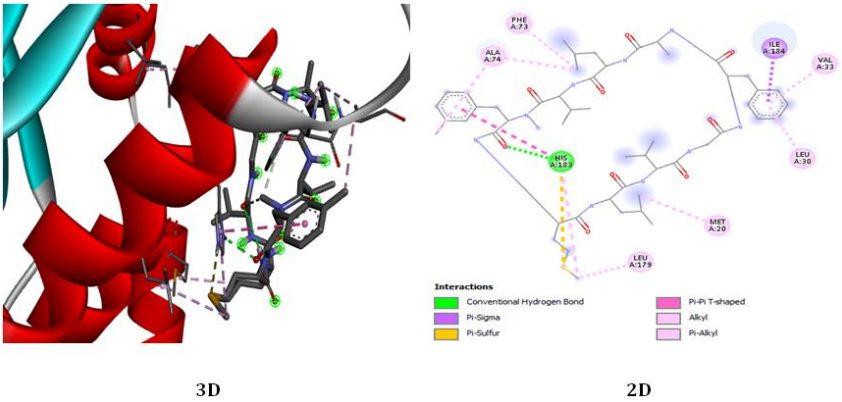

Figure 2. 2D and 3D format of docked compound **14** in Sedoheptulose-7-Phosphate Isomerase.

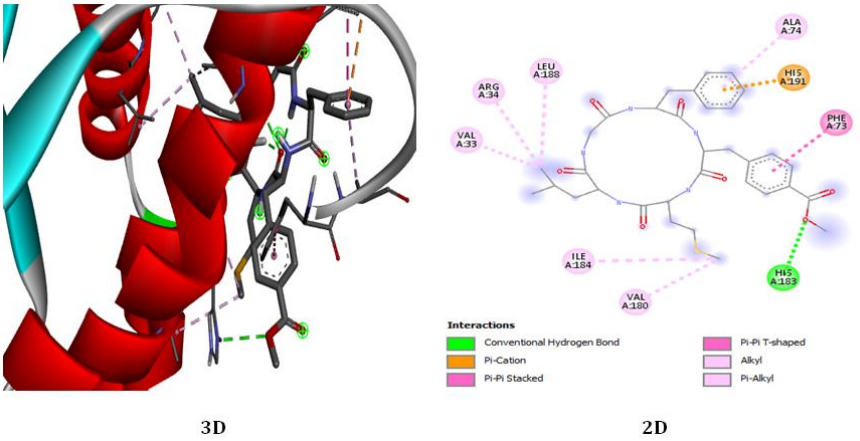

Figure 3. 2D and 3D format of docked compound **E** in Sedoheptulose-7-Phosphate Isomerase.

Molecular Dynamic Simulation Analysis

Root Mean Square Deviation

The steadiness of the studied complex is one of the key components to be investigated in molecular dynamic simulation. As observed in Figure 4, the extent of nonconformity of the investigated head-to-tail cyclic peptide (Compound 14)- sedoheptulose-7-phosphate isomerase complex and ceftazidime-sedoheptulose-7-phosphate isomerase complex to the initial structure with 100 ns simulation time were examined via root mean square deviation analysis. The configuration for compound 14- sedoheptulose-7-phosphate isomerase complex and compound **E**-sedoheptulose-7-phosphate isomerase complex, as shown in Figures 4 and 5, proved to be more stable than the configuration formed for ceftazidime- sedoheptulose-7-phosphate isomerase complex. The pattern formed by the RMSD for compound **14** and **E** (predicted compound) was irregular at the initial interaction but before 20 ns, the pattern became stable but this was not in the case of the reference drug with the receptor with red color in Figure 4. Therefore, this showed that compound **14** and **E** interacted well with the receptor thereby confirmed the ability to inhibit the target than the referenced compound (ceftazidime).

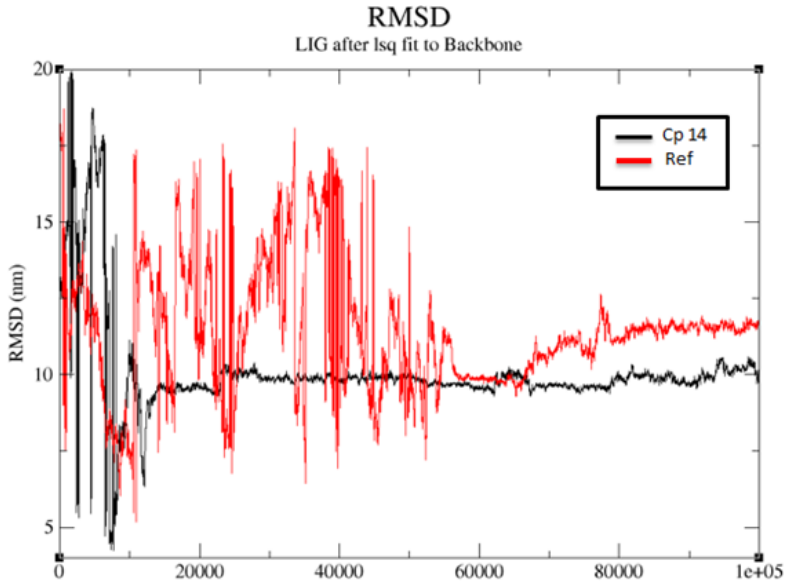

Figure 4. RMSD of Compound **14**-SPI and ceftazidime -SPI complexes during 100ns simulation.

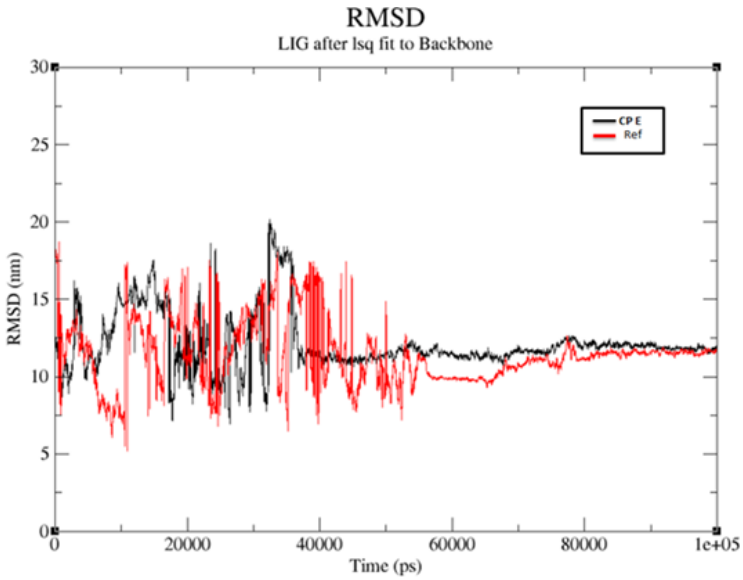

Figure 5. RMSD of compound **E**-SPI and ceftazidime -SPI complexes during 100ns simulation.

Calculated Binding Energy

The actual calculated binding energy obtained from the simulation of (3S,6S,9S,12S,18S,21S,24S,27S)-12-benzyl-6,21-diisobutyl-3,18-diisopropyl-1,9-dimethyl27-(3-methylbenzyl)-24-(2-(methylthio)ethyl)-1,4,7,10,13,16,19,22,25-nonaazacyclohep- -tacosane-2,5,8,11,14,17,20,23,26-nonaone (**14**)-sedoheptulose-7-phosphate isomerase complex and ceftazidime - sedoheptulose-7-phosphate isomerase complex are presented in Table 5. The calculated binding energy components obtained from the studied complexes were ΔE_{ele} (-0.64± 0.03 for comp14-SPI ; -0.16 ± 0.03 for comp E-SPI; 0.86±0.47 for Ref-SPI complex), ΔG_{gas} (-0.65± 0.03 for comp14-SPI complex; -0.16± 0.03 for comp E-SPI; 0.86 ± 0.47 for Ref-SPI complex), ΔG_{sol} (0.98± 0.11 for comp14-SPI complex; 0.71 ± 0.10 for comp E-SPI; -0.24 ± 0.47 for Ref-SPI

complex), and ΔG_{bind} (0.34 ± 0.11 for comp14-SPI complex; 0.55 ± 0.10 for comp E-SPI; 0.62 ± 0.08 for Ref-SPI complex) (Table 5 and Figures 6-8). The observed energetic components (electrostatic energy and gas-phase components) for compound 14-SPI complex favored the excellent inhibiting activity of compound 14 against the studied target. Oyebamiji *et al.* (2020) [41] reported that any molecule with lowest binding energy showed that it has the highest ability to inhibit the studied receptor; thus, as shown in Table 5, compound 14 proved to interact with the amino acid residue in the studied receptor far better than ceftazidime –SPI based complex and this confirmed that (3S,6S,9S,12S,18S,21S,24S,27S)-12-benzyl-6,21-diisobutyl-3,18-diisopropyl-1,9-dimethyl27-(3-methylbenzyl)-24-(2-(methylthio)ethyl)-1,4,7,10,13,16,19,22,25-nonaazacyclohep- -tacosane-2,5,8,11,14,17,20,23,26-nonaone (**14**)-sedoheptulose-7-phosphate isomerase complex proved to be a potential sedoheptulose-7-phosphate isomerase inhibitor.

Table 5. Calculated binding energy components in kcal/mol

Complexes	Binding Energy Components (kcal/mol)			
	ΔE_{ele}	ΔG_{gas}	ΔG_{sol}	ΔG_{bind}
Comp14-SPI	-0.64± 0.03	-0.65± 0.03	0.98± 0.11	0.34± 0.11
CompdE-SPI	-0.16± 0.03	-0.16± 0.03	0.71± 0.10	0.55± 0.10
REF-SPI	0.86 ±0.47	0.86 ±0.47	-0.24 ± 0.47	0.62 ±0.08

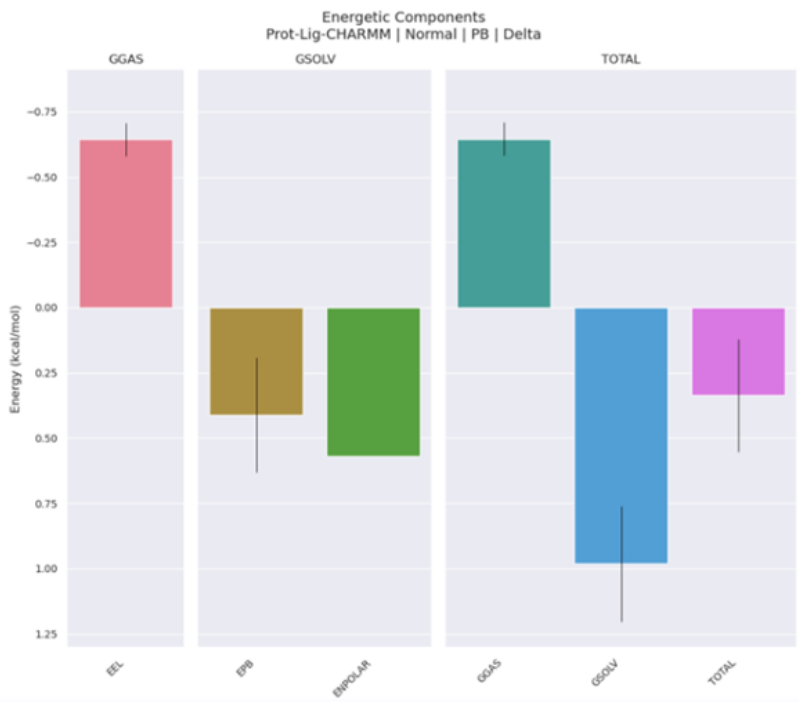

Figure 6. Chart for calculated energetic components for Comp14-SPI complex.

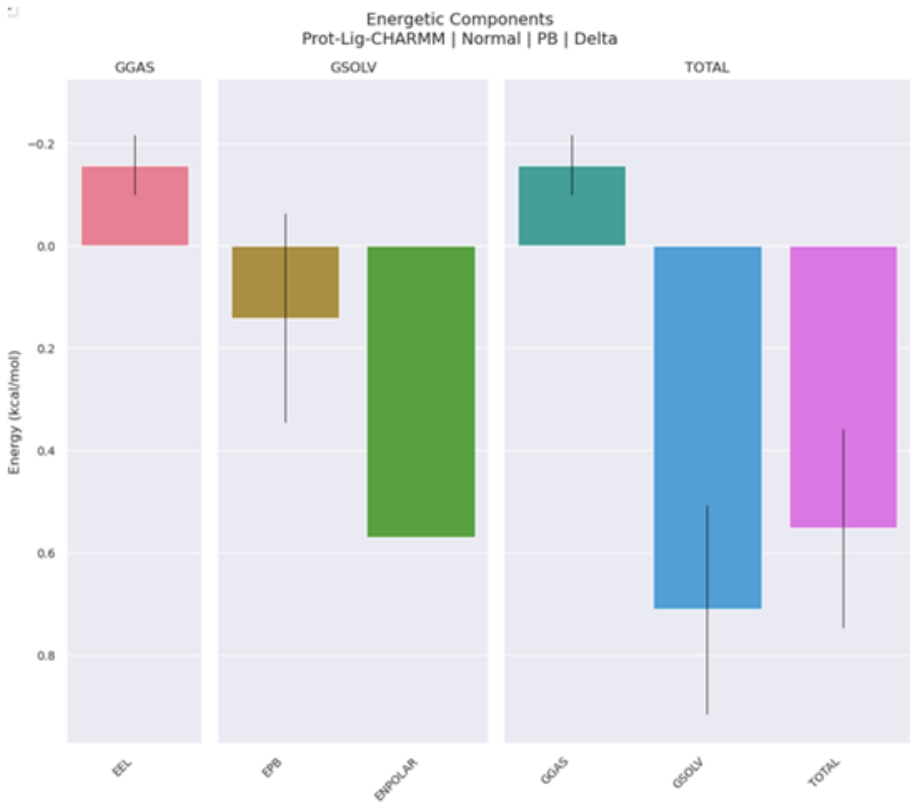

Figure 7. Chart for calculated energetic components for Cp**E**-SPI complex.

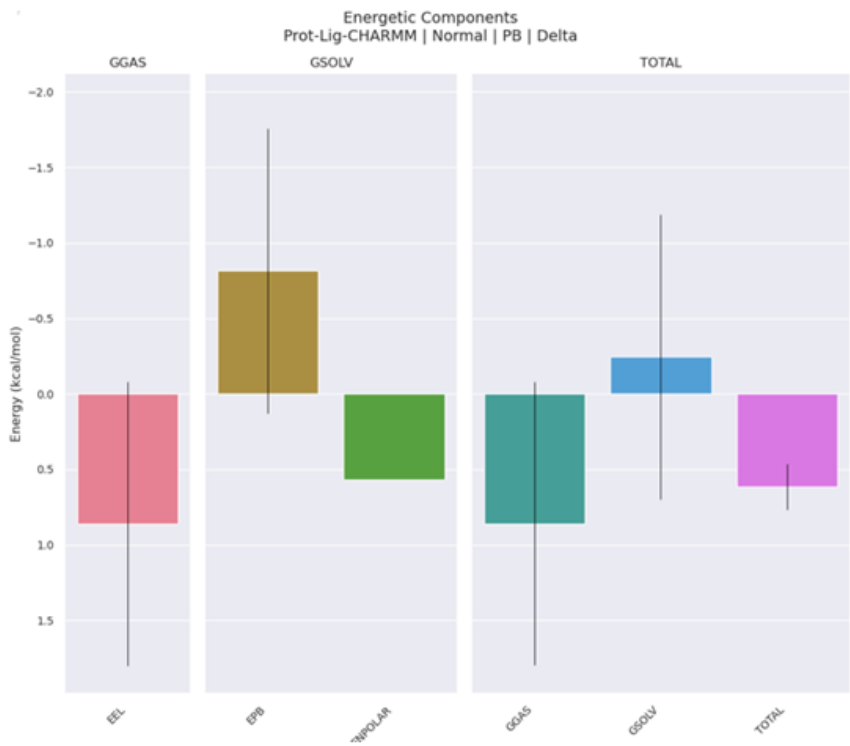

Figure 8. Chart for calculated energetic components for Ref-SPI complex.

Conclusion

Fourteen compounds were investigated via *in silico* approach. The entire compounds were optimized using Spartan software and the obtained descriptors were reported. The highest occupied molecular orbital energy (E_{HOMO}) and HOMO/LUMO energy gap (E_{LUMO} –E_{HOMO}) were observed to play a crucial role in the activity of compound **13** which thereby were observed to enhanced its inhibiting activity against sedoheptulose-7-phosphate isomerase [PDB id: 2x3y] than other studied compounds as well as ceftazidime (Reference compound). However, in this work, the potential inhibiting capacity of compound 14 with the highest binding affinity than all the studied compounds as well as the referenced molecule was established against sedoheptulose-7-phosphate isomerase [PDB id: 2x3y] via docking and molecular dynamic simulation approaches. It was observed that compound 14 showed the greater potential ability to inhibit the target and the calculated binding affinity and binding energy were -7.1 kcal/mol and 0.34$^{\pm}$ 0.11 kcal/mol respectively. Also, (3S,6S,9S,12S,18S,21S,24S,27S)-12-benzyl-6,21-diisobutyl-3,18-diisopropyl-1,9-dimethyl27-(3-methylbenzyl)-24-(2-(methylthio)ethyl)-1,4,7,10,13,16,19,22,25-nonaazacyclohep- -tacosane-2,5,8,11,14,17,20,23,26-nonaone (**14**) and ceftazidime (Reference compound) were subjected to pharmacokinetics study and it was observed that compound 14 have potential drug-capability when compared to the ADME and toxicity report for ceftazidime.

Data Availability

All data generated or analyzed during this study are included in this article and its supplementary information files.

Orcid

Oyebamiji Abel Kolawole: 0000-0002-8932-6327
Akintelu Sunday A.: 0000-0001-8919-3029
Semire Banjo: 0000-0002-4173-9165
Olanrewaju Adesoji Alani: 0000-0001-6084-4465
Akintayo Emmanuel T.: 0000-0001-8543-9554
Akintayo Cecillia O.: 0000-0003-1306-7522
Adubiaro Habibat Omolara: 0000-0001-7873-052X
Ebenezer Oluwakemi: 0000-0003-1054-9665
Babalola Jonathan O.: 0000-0002-1407-6677

References

[1] D. Dance, *Int. J. Antimicrob. Agents*, **2014**, *43*, 310-318. [CrossRef], [Google Scholar], [Publisher]

[2] C. Potisap, M.A.W. Khan, A. Boonmee, J.L. Rodrigues, S. Wongratanacheewin, R.W. Sermswan, *AMB Expr.*, **2018**, *8*, 1-14. [CrossRef], [Google Scholar], [Publisher]

[3] D. Limmathurotsakul, S. Wongratanacheewin, N. Teerawattanasook, G. Wongsu- van, S. Chaisuksant, P. Chetchotisakd, W. Chaowagul, N.P. Day, S.J. Peacock, *Am. J. Trop. Med. Hyg.*, **2010**, *82*, 1113–17. [CrossRef], [Google Scholar], [Publisher]

[4] O. Karatuna, D.A.B. Dance, E. Matuschek, J. Åhman, P. Turner, J. Hopkins, P. Amornchai, V. Wuthiekanun, T.-P. Cusack, R. Baird, J. Hennessy, R. Norton, M. Armstrong, S. Zange, L. Zoeller, T. Wahab, D. Jacob, R. Grunow, G. Kahlmeter. *Clin. Microbiol. Infect.*, **2021**, *27*, 736e741. [CrossRef], [Google Scholar], [Publisher]

[5] Y.C. Chee, *Radiol. Infect. Dis.*, **2020**, *7*, 31e34. [CrossRef], [Google Scholar], [Publisher]

[6] R. Seng, R. Phunpang, N. Saiprom, A. Dulsuk, C. Chewapreecha, J. Thaipadungpanit, EM. Batty, W. Chantratita, TE West, N Chantratita. *Front. Microbiol.* **2023**, *14*, 1103297. [CrossRef], [Google Scholar], [Publisher]

[7] V.K. Paul, A. Govindakarnavar, T. Meghan, L. Mark, S. Nalini, *Asian Pac. J. Trop. Med.*, **2016**, *9*, 515–524. [CrossRef], [Google Scholar], [Publisher]

[8] M.S. Kim, D.H. Shin, *Acta Crystallogr. F:Struct. Biol. Commun.*, **2009**, *65*, 1110-1112. [CrossRef], [Google Scholar], [Publisher]

[9] N.J. Harmer, *J. Mol. Biol.*, **2010**, *400*, 379-392. [CrossRef], [Google Scholar], [Publisher]

[10] C. Potisap, M.A.W. Khan, A. Boonmee, J.L. Rodrigues, S. Wongratanacheewin, R.W. Sermswan, *AMB Express*, **2018**, *8*, 136. [CrossRef], [Google Scholar], [Publisher]

[11] P.L. Taylor, K.M. Blakely, G.P. De Leon, J.R. Walker, F. McArthur, E. Evdokimova, K. Zhang, M.A. Valvano, G.D. Wright, M.S. Junop, *J. Biol. Chem.*, **2008**, *283*, 2835-2845. [CrossRef], [Google Scholar], [Publisher]

[12] M.J. Anderson, T.O. Crist, J.M. Chase, M. Vellend, B.D. Inouye, A.L. Freestone, N.J. Sanders, H.V. Cornell, L.S. Comita, K.F. Davies, *Ecol. Lett.*, **2011**, *14*, 19-28. [CrossRef], [Google Scholar], [Publisher]

[13] P. Boottanun, C. Potisap, J.G. Hurdle, R.W. Sermswan, *AMB express*, **2017**, *7*, 16. [CrossRef], [Google Scholar], [Publisher]

[14] M.A. Abdalla, L.J. McGaw, *Molecules*, **2018**, *23*, 2080. [CrossRef], [Google Scholar], [Publisher]

[15] X. Jing, K. Jin, *Med. Res. Rev.*, **2020**, *40*, 753–810. [CrossRef], [Google Scholar], [Publisher]

[16] T. Mogi, K. Kita, *Cell. Mol. Life Sci*. **2009**, *66*, 3821–3826. [CrossRef], [Google Scholar], [Publisher]

[17] F. Román-Hurtado, M. Sánchez-Hidalgo, J. Martín, F.J. Ortiz-López, D. Carretero-Molina, F. Reyes, O. Genilloud, *Microorganisms*, **2021**, *9*, 135. [CrossRef], [Google Scholar], [Publisher]

[18] N.J. Harmer, *J. Mol. Biol.*, **2010**, *400*, 379. [CrossRef], [Google Scholar], [Publisher]

[19] G. Li, F. Yuan, B. Yao, *Org. Lett.* **2022**, 24, *31*, 5767–5771. [CrossRef], [Google Scholar], [Publisher]

[20] A.K. Oyebamiji, J.O. Babalola, K.A. Odelade, S.A. Akintelu, O.A. Nubi, H.O. Aworinde, E. Faboro, E.T. Akintayo, B. Semire, *Eclét. Quím.*, **2023**, *48*, 54-80. [CrossRef], [Google Scholar], [Publisher]

[21] E. Pakizeh, M. Mohammadi, A. Mostafaei, *Solid State Commun.*, **2023**, *369*, 115214. [CrossRef], [Google Scholar], [Publisher]

[22] M. Mohammadi, E. Pakizeh, *Chin. J. Phys.*, **2023**, *In press*. [CrossRef], [Google Scholar], [Publisher]

[23] M. Mohammadi, E. Pakizeh, *Mater. Sci. Eng. B*, **2023**, *297*, 116752. [CrossRef], [Google Scholar], [Publisher]

[24] D. Jacquemin, E.A. Perpe`te, I. Ciofini, C. Adamo, *Acc. Chem. Res.*, **2008**, *42*, 326. [CrossRef], [Google Scholar], [Publisher]

[25] M. Pastore, E. Mosconi, F. de Angelis, M. Gratzel, *J. Phys. Chem. C*, **2010**, *114*, 7205-7212. [CrossRef], [Google Scholar], [Publisher]

[26] F. Iorhuna, A.A. Muhammad, T.A. Nyijime, M. Shuaibu. *Adv. J. Chem. A*, **2023**, *6*, 380-390. [CrossRef], [Publisher]

[27] S. Hadidi, M.H. Farzaei. *Adv. J. Chem. A*, **2023**, *6*, 123-140. [CrossRef], Publisher]

[28] J.P. Ameji, A.O. Ebune, I.W. Aderemi, A. Moyosore, G. Idah. *Adv. J. Chem*. A, **2023**, *6*, 92-104. [CrossRef], [Google Scholar], [Publisher]

[29] A.K. Oyebamiji, E.T. Akintayo, C.O. Akintayo, H.O. Aworinde, O.D. Adekunle, S.A. Akintelu, *Ukr. Biochem. J.* **2023**, *95*, 93-105. [CrossRef], [Google Scholar], [Publisher]

[30] B. Semire, A.K. Oyebamiji, O.A. Odunola, *Sci. Afr.,* **2020**, *7*, e00287. [CrossRef], [Google Scholar], [Publisher]

[31] M. Abdul-Hammed, B. Semire, SA Adegboyega, AK Oyebamiji, T.A. Olowolafe. *Phys. Chem. Res.,* **2020**, *8*, 296-310. [CrossRef], [Google Scholar], [Publisher]

[32] R.O. Oyewole, A.K. Oyebamiji, B. Semire, *Heliyon*, **2020**, *6*, e03926. [CrossRef], [Google Scholar], [Publisher]

[33] R.O. Adegoke, A.K. Oyebamiji, B. Semire, *Data Brief,* **2020**, *31*, 105963. [CrossRef], [Google Scholar], [Publisher]

[34] U.A. Çevik, I. Celik, A. Işık, R.R. Pillai, T.E. Tallei, R. Yadav, Y. Özkay, Z.A. Kaplancık, *J. Mol. Struct.* **2022**, *1252*, 132095. [CrossRef], [Google Scholar], [Publisher]

[35] H.A. Radwan, I. Ahmad, SR. Akand, M. Shaikh, R. Pawara, SN. Manjula, H. Patel, *J. Mol. Struct.* **2022**, *1251*, 131972. [CrossRef], [Google Scholar], [Publisher]

[36] D.R. Roe, T.E. Cheatham III, *J. Chem. Theory Comput.*, **2013**, *9*, 3084–3095. [CrossRef], [Google Scholar], [Publisher]

[37]. M.D. Adeoye, A.K. Oyebamiji, M.A. Ashiru, R.A. Adigun, O.H. Olalere, B. Semire, *Eclet. Quim. J.*, **2022**, *47*, 27-36. [CrossRef], [Google Scholar], [Publisher]

[38] S. A. Jamelah, H.A. Aljawhara, Y.S. Mary, Y.S. Mary, *J. Mol. Struct.,* **2020**, *1217*, 128388. [CrossRef], [Google Scholar], [Publisher]

[39] B. Semire, A. Oyebamiji, M. Ahmad, *Pak. J. Chem.,* **2012**, *2*, 166-173. [Google Scholar], [Publisher]

[40] E.A. Erazua, S.A. Akintelu, J.M. Adelowo, S.N. Odoemene, O.M. Josiah, S.F. Raheem, D.F. Latona, M.D. Adeoye, A.O. Esan, A.K. Oyebamiji, *Trop. J. Nat. Prod. Res.*, **2021**, *5*, 2022-2029. [CrossRef], [Google Scholar]

[41] A.K. Oyebamiji, G.F. Tolufashe, O.M. Oyawoye, T.A. Oyedepo, B. Semire, *J. Chem.*, **2020**, 6735232. [CrossRef], [Google Scholar], [Publisher]

HOW TO CITE THIS ARTICLE

Abel Kolawole Oyebamiji*, Sunday A. Akintelu, Banjo Semire, Adesoji Alani Olanrewaju, Emmanuel T. Akintayo, Cecillia O. Akintayo, Habibat Omolara Adubiaro, Oluwakemi Ebenezer, Jonathan O. Babalola. Molecular Modeling Insights into Bioactivities of Head-to-Tail Cyclic Peptides: Potential Sedoheptulose-7-Phosphate Isomerase Inhibitors. *Adv. J. Chem. A*, 2024, 7(2), 146-162.

DOI: 10.48309/ajca.2024.418437.1426
URL: https://www.ajchem-a.com/article_183938.html